Sensitivity Improved Surface Plasmon Resonance Biosensor for Cancer Biomarker Detection Based on Plasmonic Enhancement

Wing-Cheung Law,[†,§] Ken-Tye Yong,[†,‡,§] Alexander Baev,[†] and Paras N. Prasad[†,§,*]

[†]Institute for Lasers, Photonics and Biophotonics, State University of New York at Buffalo, Buffalo, New York 14260-3000, United States, [‡]School of Electrical and Electronic Engineering, Nanyang Technological University, Singapore 639798, Singapore, and [§]International Joint Research Center for Nanophotonics and Biophotonics, Changchun, Jilin 130022, China

ABSTRACT In this study, we report the development of a nanoparticle-enhanced biosensor by integrating both the nanoparticles and immunoassay sensing technologies into a phase interrogation surface plasmon resonance (SPR) system for detecting antigen at a concentration as low as the femtomolar range. Our work has demonstrated that the plasmonic field extension generated from the gold film to gold nanorod (GNR) has led to a drastic sensitivity enhancement. Antibody-functionalized sensing film, together with antibody-conjugated GNRs, was readily served as a plasmonic coupling partner that can be used as a powerful ultrasensitive sandwich immunoassay for cancer-related disease detection. Experimentally, it was found that the bioconjugated GNR labels enhance the tumor necrosis factor alpha (TNF-α) antigen signal with more than 40-fold increase compared to the traditional SPR biosensing technique. The underlying principle was analyzed by simulating the near-field coupling between the sensing film and the GNR. The results have shown that GNRs were readily served as promising amplification labels in SPR sensing technology.

KEYWORDS: gold nanorod · surface plasmon resonance · biosensor · TNF-α

Surface plasmon resonance biosensors have become an indispensable tool for studying biomolecular interactions in pharmaceutical and biomedical research over the past decade.[1,2] By detecting a small refractive index change at the metal/analyte interface, the information of the biomolecular interactions can be obtained by measuring the optical characteristics (intensity, phase, and polarization) of light reflected from the optical setup, usually a Kretschmann configuration.[3−9] SPR has become a prominent sensing technique with numerous applications because of the capability of real-time monitoring analyte−analyte interactions with high sensitivity.[10,11] In a SPR-based biosensor, an extremely small amount of analyte is subjected to interact with the sensing surface where the specific biomolecular receptors were immobilized. In typical SPR systems, the information of biomolecular interaction was obtained from monitoring the change of resonance angle or wavelength.[3,12−16] Although such technologies have successfully demonstrated high detection sensitivity in the range of picomolar of analyte, small molecules such as DNA and cytokine have been difficult to be detected using the current setup.

Recent developments of nanomaterials have remarkably enhanced the detection sensitivities of biosensors. For example, the use of nanoparticles in electrochemiluminescence-based biosensors exhibits many advantages over the traditional organic dye.[17,18] The detection limit and the diversity of fluorescence-based biosensors have been improved using both organic and inorganic nanomaterials.[19] A lot of attention has been focused on the exploitation of metallic nanoparticles in sensing applications because of the extremely sensitive nature of their electron-rich surfaces to the surrounding environment. When an electromagnetic wave is directed to the metallic nanoparticle, an induced oscillation of free electrons (plasmons) occurs at the surface. This phenomenon has rendered the outstanding development of localized surface plasmon resonance (LSPR)-based and surface-enhanced Raman scattering (SERS)-based biosensors that are based on monitoring the extinction spectra of nanoparticles or, more specifically, the position of peak wavelengths obtained in absorbance and Raman measurements.[20−22] However, there are few reports that utilize this unique property of metallic nanoparticle as a signal amplification strategy.[23−29] In fact, the potential of using metallic nanoparticles in SPR sensors was explored by Natan's group in

* Address correspondence to pnprasad@buffalo.edu.

Received for review March 12, 2011 and accepted April 21, 2011.

Published online April 21, 2011
10.1021/nn2009485

TABLE 1. Summary of Au-Amplified SPR Assay Development

SPR interrogation system	enhancement strategy	particle diameter	analyte	sensitivity (pM)	ref
angular reflectivity	colloidal Au nanoparticle	~11 nm	human IgG antibody	6.7	23
angular reflectivity	colloidal Au nanoparticle	~12 nm	oligonucleotide	10	24
angular reflectivity	colloidal Au nanoparticle	~9 nm	oligonucleotide	1	26
angular reflectivity	colloidal Au NP, dextran matrix	not mentioned	oligonucleotide	1.38	27
angular reflectivity	colloidal Au nanoparticle	~15 nm	carbamate inhibitors	7–12	28
phase	colloidal Au nanorod	~48 × 22 nm	TNF-α antigen	0.03	current work

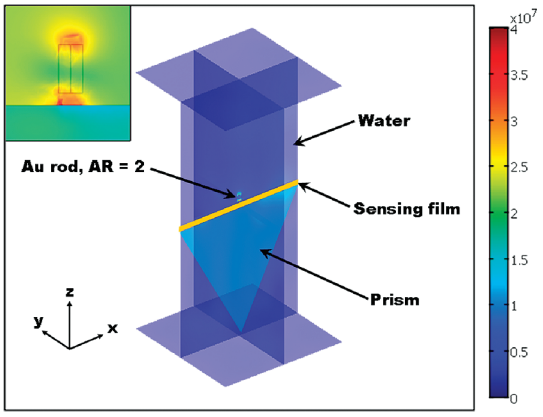

Figure 1. Norm of the electric field in planes, outlining the solution space. The gold nanorods with AR = 2 are pointed to by the arrow.

1999.[30] They found that the metallic nanoparticles induced the increase in binding mass, the increase in refractive index, and the perturbation of evanescent field that led to enhanced sensitivity. Typically, two strategies were employed for the Au-amplified SPR biosensors: (i) targeted analyte is directly conjugated to the gold nanoparticle, and the whole conjugate is flowed through the sensing surface (direct binding); and (ii) targeted analyte was flowing through the sensing surface followed by a secondary nanoparticle conjugate that binds to the captured analyte (sandwich assay). In practical means, the second approach will be more preferable because the premodification of the analyte could be omitted. Development over the past decade of a Au-amplified SPR biosensor is summarized in Table 1. One can observe that most of the nanoparticle-based SPR biosensors were based on a spherical particle and angular reflectivity interrogation system. Although high detection sensitivity (picomolar range) and low molecular weight analyte detection had been demonstrated, detection sensitivity and specificity should be further improved, especially for the detection of small molecules in cancer diagnosis applications.

In our previous studies, SPR phase shift was monitored in our setup, which has been recognized as higher detection sensitivity because of the steep phase jump behavior in resonant conditions.[31,32] In addition, GNR labels are more favorable to the Au-amplified SPR biosensors because of the unique behavior of GNRs, the tunable longitudinal plasmonic peak which enables an effective plasmonic coupling between sensing film and nanoparticle.[33] In this work, we reveal the potential of applying this "perfectly matched" nanotag in a well-established SPR sensing system and immunoassay. Through the detection of tumor necrosis factor alpha (TNF-α) antigen, we observed 40-fold sensitivity enhancement using wavelength-matched GNRs. As shown in Table 1, the detection sensitivity of TNF-α was estimated to be 0.03 pM (molecular weight of TNF-α ~17 kDa), which is about 1–2 orders of magnitude higher than the traditional immunoassay method. SPR biosensors have been utilized in different fields ranging from medical, food safety, to homeland security.[5] A simple, yet efficient strategy, which can be quickly adapted to the well-established setup, should be developed to satisfy the high demand of high sensitivity and time-efficient biosensors. Our results provide a prospective development of the next generation SPR biosensor technology using metallic labels for sensitivity improvement.

RESULTS AND DISCUSSION

Simulation. COMSOL Multiphysics 3.5 was used to simulate near-field coupling between the sensing film and nanorod labels. Full-wave 3D analysis was employed with scattered electric field formulation. Solution space of 1 μm × 1 μm × 2 μm (Figure 1) was encaged in PML subdomains with scattering boundary conditions imposed on all outer boundaries. The nanorod is represented by a solid gold cylinder with the radius of 10 nm and different heights, corresponding to different computed aspect ratios (ARs). The gold dielectric function was adopted from Etchegoin *et al.*[34] The incident electric field was set in spherical coordinates with azimuthal and polar angles defining components of the wave and polarization vectors. As shown in the inset of Figure 1, the coupling field was localized at the tips of GNRs.

The results of our simulations are presented in Figure 2. In Figure 2a, the norm of the electric field is plotted *versus* the distance from the glass substrate (prism) for a simulation with the aspect ratio of the GNR equal to 2 (40 nm × 20 nm). The sensing film was set as 50 nm thick. We simulated a laser light (785 nm) coming from the left-hand side and hitting the film at "0" nm of the *x*-axis. The plotted values were measured from the

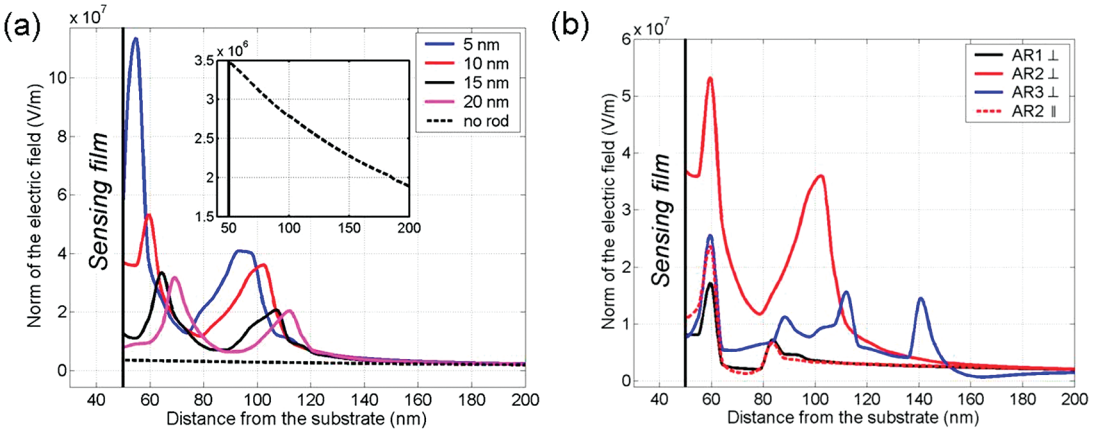

Figure 2. Norm of the electric field representing (a) different distance between GNR with AR2 and the sensing film, and (b) different ARs and orientations of GNR 10 nm away from the sensing film.

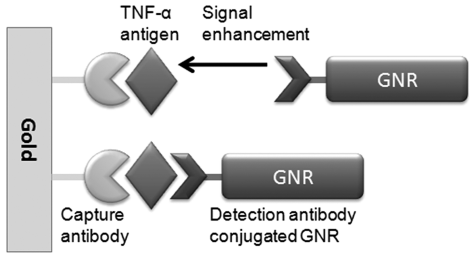

Scheme 1. Schematic diagram of an ultrasensitive immunoassay based on using GNR as an amplification label.

top of the sensing film ("50" nm of the *x*-axis) to the edge of the GNRs that perpendicularly aligned against the film. It should be noted that, without the GNR perturbation, the field is relatively weak and exponentially decreases with the distance from the film (black dotted line). In the inset of Figure 2a, it is shown that the field is confined in the range of ~150 nm from the film. As the sensing capability is limited in this region, any perturbation of evanescent field could potentially lead to a signal enhancement and higher detection sensitivity. By introducing GNR to this region, the evanescent field coupling between sensing film and GNR results in excitation of longitudinal plasmon mode of the GNR and corresponding huge increase of local field at the tips of GNRs. Figure 2a shows the field intensities at the tips of the GNR with different distances away from the sensing film. The simulation result shows the largest increase of local field when the distance between GNR and sensing film is 5 nm. In addition, Figure 2b illustrates that the responses correspond to different aspect ratios and orientation of the GNR for a fixed distance (10 nm) between the GNR and the film. The excitation of longitudinal plasmon mode is most effective for the GNR oriented perpendicularly to the film and with AR = 2, where the surface plasmon wavelength matches the localized surface plasmons of the GNR. On the basis of these simulations, we hypothesize that the perturbation of the evanescent field originating from the GNRs could potentially generate a pronounced SPR signal in the reflected light and lead to sensitivity enhancements.

SPR Measurement. The simulated hypothesis was examined experimentally using our phase-sensitive SPR setup.[31] Scheme 1 shows our idea of utilizing GNR conjugates as the secondary "labels" in a SPR-based sandwich immunoassay. As shown in Scheme 1, the sensing film surface is first prepared with capture antibodies. Then the antigen-containing solution, which is highly specific to the capture antibodies, will be applied to the surface. An exponential binding curve would be expected in the SPR sensorgram, indicating that the specific binding interaction occurs between antigen and antibody. The addition of detection antibody-conjugated GNRs, which bind the antigen to a different epitope than the capture antibody, will lead to the "secondary" response and result in sensitivity enhancement. To demonstrate the capability and feasibility of a GNR-amplified biosensor for clinical application, we conducted a TNF-α antigen (TNF-α) detection using a sandwich immunoassay strategy. TNF-α is a well-studied mediator of inflammatory and immunodefense function. The concentration of TNF-α was found to be higher in inflammation, bacterial infection, and nonhealing wounds.[35] It was also recognized as a tumor promoter that may be involved in a tumor initiation process.[36] However, the concentration of TNF-α in biological fluid is very low (~20 pg/mL in a healthy person).[37] Thus, an ultrasensitive biosensor is essential for monitoring the concentration of this biomarker, which may potentially serve as a diagnostic tool for early detection of cancer. We demonstrate the capability of our biosensor by modifying the sensing film with monoclonal anti-human TNF-α antibody (cAb) solution and conjugating anti-human TNF-α antibody (dAb) to GNR-645 (GNR-Ab). Thus, cAb-modified sensing film together with GNR-Ab can serve as an ultrasensitive tool for TNF-α antigen detection, as schematically presented in Scheme 1. Basically, the enhancement was accomplished by

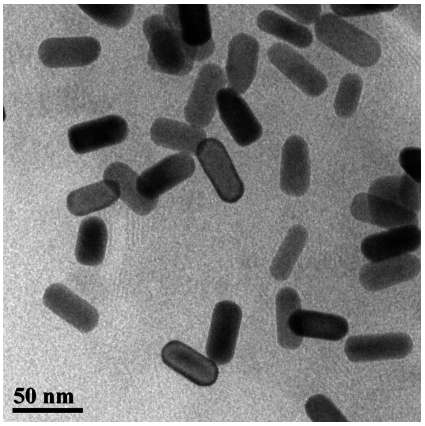

Figure 3. TEM picture of GNR with the LSPR peak at 645 nm.

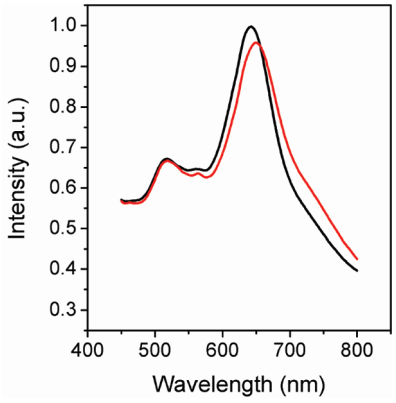

Figure 4. Absorption spectra of GNRs (black curve) and dAb-conjugated GNRs (red curve).

secondary binding of GNR-Ab to the captured TNF-α antigen (targeted analyte) that led to a larger perturbation of the SPR condition.

Figure 3 shows a TEM image of the GNR that was used in our studies. The average dimension of the GNRs was estimated to be 46.5 ± 2.9 nm long and 21.1 ± 1.8 nm wide, which represents an aspect ratio of 2.20. This feature can be also characterized by the longitudinal peak in the absorption spectrum. As shown in Figure 4 (black curve), a dominant, sharp, and narrow absorption band was observed at 645 nm (GNR-645), indicating the high yield and the high monodispersity of GNRs. In our previous studies, we found that maximum sensing enhancement can be achieved when the plasmonic behavior of the gold nanotag matches the operating wavelength of the laser source. Thus, GNR-645 was chosen as the amplifying label in our experiments as its aspect ratio is close to 2 and it matches with the 785 nm laser source.[33]

As shown in Scheme 2, the dAbs were conjugated to the GNRs' surface by electrostatic force between the positively charged CTAB and the negative charge contributed by the carboxyl groups in the Fc region of antibodies.[38] It should be noted that the concentration of dAb solution applied in our protocol is

Scheme 2. Bioconjugation of GNRs by electrostatic attraction.

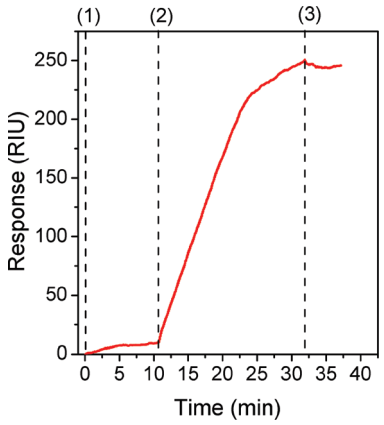

Figure 5. Real-time response curve corresponds to the immunoassay illustrated in Scheme 2: (1) TNF-α (5 ng/mL), (2) dAb-conjugated GNR solution, and (3) PBS.

much higher than the GNR solution in order to ensure a complete coverage of the GNR surface. Unreacted dAbs were removed by centrifugation. Figure 4 shows the absorption spectra of GNR solution before and after bioconjugation (GNR-Ab). The longitudinal plasmonic peak of GNR solution was shifted by 6 nm, which can be attributed to the change of localized refractive index near the GNR surface, indicating that the dAbs were successfully attached to the GNR surface.

The concept of Scheme 1 is exhibited in Figure 5. In Figure 5, the baseline was initially set by running PBS on the cAb-functionalized sensing film for 1−2 min. A PBS buffer containing TNF-α (5 ng/mL) was then introduced into the sensor head. As given in Figure 5, there is a significant change in the SPR signal when TNF-α reacts with the cAb. After the signal reached a plateau, the PBS was introduced again to remove unreacted TNF-α. Subsequently, the system was exposed to the GNR-Ab solution and led to another dramatic change of the signal. It is worth mentioning that this dramatic change is due to the binding reaction between the immobilized TNF-α and dAb on the GNR surface. The signal did not backshift after rinsing the surface with PBS, which confirms the binding reaction. In addition, a control experiment was conducted under the same conditions but without the exposure of TNF-α. The data show much less reactivity between cAb and dAb (see Figure 6), suggesting that the detected signal was obtained from a highly specific immunoassay rather than a nonspecific binding reaction.

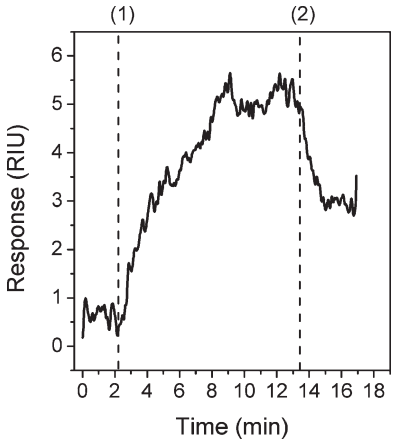

Figure 6. Real-time response curve corresponds to the nonspecific binding between cAb-sensing film and dAb-GNR: (1) dAb-conjugated GNR solution and (2) PBS.

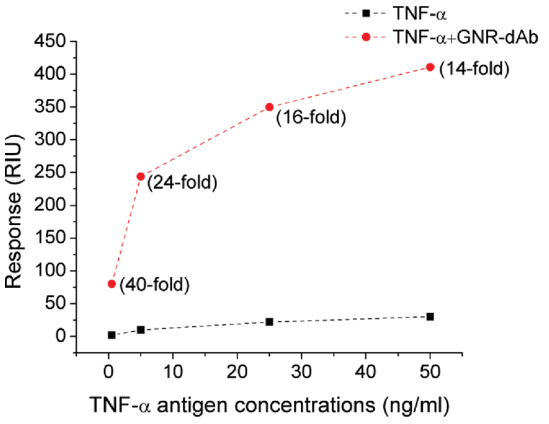

Figure 7. Response and magnitude of enhancement (in the blanket) obtained from the sandwich immunoassay with (●) and without (■) exposing the sensing film to the GNR-Ab solution after TNF-α.

To fully explore the potential of this ultrasensitive assay, a systematic study was carried out by exposing the cAb-modified sensing films to different concentrations of TNF-α (0.5, 5, 25, and 50 ng/mL) accompanied with the GNR label. The result (■) shown in Figure 7 indicates that the unit changes due to these extremely small amounts of antigens were 2 to 30 units. Although the detection limit readily reaches the nanogram/milliliter range, it can be further improved by introducing an amplification label in each of the binding events. As shown in Figure 7 (●), exposing the sensing film to GNR-Ab after TNF-α yielded a dramatic enhancement of signal. The use of GNR-Ab as an amplification label in this sandwich immunoassay permitted 14−40-fold increase in sensitivity. It is worth mentioning that a larger enhancement was observed at low concentration detection and *vice versa*. We believe that this concentration-dependent phenomenon can be accounted for by the nonlinear phase response under SPR conditions.[39−42] The lowest detectable concentration of TNF-α was 0.5 ng/mL (0.03 pM), and the signal can be further enhanced 40-fold using GNR-Ab amplification labels. We believe that the 40-fold increase in sensitivity should enable one to monitor a relatively low concentration of TNF-α variation, which could be one of the important indicating parameters for early cancer detection.

CONCLUSION

In our work, we have demonstrated GNR as the amplification label for a SPR-based biosensor. There are three crucial components in this unique setup: (i) highly specific "capture" sensing film, (ii) sensitive interrogation setup, and (iii) wavelength-matched Au nanotag. We have shown that the strategy for utilizing GNR conjugates together with our phase-sensitive setup led to a 1−2 orders of magnitude better detection sensitivity than that with the conventional setups. We believe that the achieved detection sensitivity, 0.03 pM, should be sufficient (i) to monitor small variation of TNF-α, (ii) to understand the cancer biology, and (iii) to investigate the progress of any therapeutic drug treatment. More importantly, this study only presents one example of incorporating GNRs in an oncology biosensor. Nevertheless, the same strategy can be applied to monitor a wide range of biomolecular interactions using a SPR-based device.

METHODS

Materials. A glass slide with a 50 nm thick gold coating was purchased from Platyus Technologies. 3-Mercaptopropionic acid (MPA), *N*-hydroxysuccinimide (NHS), ethyl-3-(3-dimethylaminopropyl)carbodiimide hydrochloride (EDC), cetyltrimethyl ammonium bromide (CTAB), silver nitrate ($AgNO_3$), sodium borohydride ($NaBH_4$), ascorbic acid, and gold(III) chloride trihydrate ($HAuCl_4$) were obtained from Sigma-Aldrich and used as received. Tumor necrosis factor-alpha (TNF-α) antigen, monoclonal anti-human TNF-α antibody (capture antibody, cAb), and anti-human TNF-α antibody (detector antibody, dAb) were obtained from R&D System, Inc.

Synthesis of Gold Nanorods (GNRs). The GNRs were prepared by the seed-mediated growth method in CTAB surfactant solution as previously described.[43] Briefly, 400 μL of 25 mM $HAuCl_4$ and 10 mL of HPLC-grade water were added to 200 μL of 4.0 mM $AgNO_3$ solution in a water bath at 35 °C. Then, 10 mL of 0.2 M CTAB and 400 μL of 0.08 M ascorbic acid were added to this solution. The solution became clear and colorless after gently stirring. We refer to this as growth solution. The seed solution was prepared by mixing 5 mL of 0.2 M CTAB solution and 5 mL of 0.96 mM $HAuCl_4$. Then 0.6 mL of ice-cold 0.01 M $NaBH_4$ solution was quickly added and vigorously stirred for 2 min. Then, 48 μL of seed solution was added to the growth solution. The resulting mixture was left undisturbed for 24 h in the water bath. GNRs were purified from the excess surfactant solution by centrifugation (13 000 rpm for 15 min).

Preparation of dAb-Conjugated GNR. Bioconjugation of GNRs to dAb was carried out as reported.[38] In brief, GNR solution was diluted to the optical density value of the longitudinal peak of GNR to 0.30 (stock solutions). Then 100 μL of GNR stock solution

was added dropwise to 100 μL of 250 μg/mL dAb solution in PBS. The mixture was shaken gently and left for 15−30 min. The GNR-Ab conjugates were purified by centrifugation to remove excess dAb and redispersed in 1 mL of PBS.

Functionalization of SPR Sensing Film. The sensing film was first immersed in a 20 mM MPA solution overnight in order to modify the Au surface with carboxyl functional groups. Then the carboxyl groups were activated by carbodiimide cross-linker, EDC, forming an amine-reactive intermediate with NHS. The mixture of EDC and NHS with a molar ratio of 1:1 was added to the carboxylated surface for 30 min and then rinsed with buffer solution. Then the sensing film was attached to the flow cell with an estimated exposure surface area of 0.5 cm^2. The cAb solution (500 μg/mL) was incubated in the flow cell for 30 min to allow the intermediate to react with the amine groups on antibodies. The flow cell was subsequently rinsed with buffer solution for 5 min to wash out unreacted antibodies.

Instrumentation. All of the SPR signals we measured are based on our home-designed SPR biosensor, where the phase (third harmonic signal) change was monitored. Detailed schematic diagram description can be found in ref 31. Transmission electron microscopy (TEM) images were obtained using a JEOL model JEM-100CX microscope with an acceleration voltage of 100 kV. The UV/vis absorption spectra of GNRs were acquired at room temperature by using a Shimadzu UV-3600 spectrophotometer.

Acknowledgment. The authors are grateful for the support from the John R. Oishei Foundation and the start-up grant of the International Joint Research Center for Nanophotonics and Biophotonics.

REFERENCES AND NOTES

1. Prasad, P. N. *Nanophotonics*; Wiley-Interscience: New York, 2003.
2. Prasad, P. N. *Introduction to Biophotonics*; Wiley-Interscience: New York, 2003.
3. Akimoto, T.; Ikebukuro, K.; Karube, I. A Surface Plasmon Resonance Probe with a Novel Integrated Reference Sensor Surface. *Biosens. Bioelectron.* **2003**, *18*, 1447–1453.
4. Chien, F. C.; Chen, S. J. A Sensitivity Comparison of Optical Biosensors Based on Four Different Surface Plasmon Resonance Modes. *Biosens. Bioelectron.* **2004**, *20*, 633–642.
5. Homola, J. Surface Plasmon Resonance Sensors for Detection of Chemical and Biological Species. *Chem. Rev.* **2008**, *108*, 462–493.
6. Markowicz, P. P.; Law, W. C.; Baev, A.; Prasad, P. N.; Patskovsky, S.; Kabashin, A. Phase-Sensitive Time-Modulated Surface Plasmon Resonance Polarimetry for Wide Dynamic Range Biosensing. *Opt. Express* **2007**, *15*, 1745–1754.
7. Wang, T.-J.; Hsieh, C.-W. Surface Plasmon Resonance Biosensor based on Electro-optically Modulated Phase Detection. *Opt. Lett.* **2007**, *32*, 2834–2836.
8. Wu, S. Y.; Ho, H. P.; Law, W. C.; Lin, C.; Kong, S. K. Highly Sensitive Differential Phase-Sensitive Surface Plasmon Resonance Biosensor Based on the Mach-Zehnder Configuration. *Opt. Lett.* **2004**, *29*, 2378–2380.
9. Nelson, S. G.; Johnston, K. S.; Yee, S. S. High Sensitivity Surface Plasmon Resonace Sensor Based on Phase Detection. *Sens. Actuators, B* **1996**, *35*, 187–191.
10. Ho, H. P.; Law, W. C.; Wu, S. Y.; Lin, C.; Kong, S. K. Real-Time Optical Biosensor Based on Differential Phase Measurement of Surface Plasmon Resonance. *Biosens. Bioelectron.* **2005**, *20*, 2177–2180.
11. Piliarik, M.; Vaisocherová, H.; Homola, J. A New Surface Plasmon Resonance Sensor for High-Throughput Screening Applications. *Biosens. Bioelectron.* **2005**, *20*, 2104–2110.
12. Ho, H. P.; Wu, S. Y.; Yang, M.; Cheung, A. C. Application of White Light-Emitting Diode to Surface Plasmon Resonance Sensors. *Sens. Actuators, B* **2001**, *80*, 89–94.
13. Nakagawa, H.; Saito, I.; Chinzei, T.; Nakaoki, Y.; Iwata, Y. The Merits/Demerits of Biochemical Reaction Measurements by SPR Reflectance Signal at a Fixed Angle. *Sens. Actuators, B* **2005**, *108*, 772–777.
14. Piliarik, M.; Vala, M.; Tichý, I.; Homola, J. Compact and Low-Cost Biosensor Based on Novel Approach to Spectroscopy of Surface Plasmons. *Biosens. Bioelectron.* **2009**, *24*, 3430–3435.
15. Shumaker-Parry, J. S.; Aebersold, R.; Campbell, C. T. Parallel, Quantitative Measurement of Protein Binding to a 120-Element Double-Stranded DNA Array in Real Time Using Surface Plasmon Resonance Microscopy. *Anal. Chem.* **2004**, *76*, 2071–2082.
16. Yuk, J. S.; Kim, H.-S.; Jung, J.-W.; Jung, S.-H.; Lee, S.-J.; Kim, W. J.; Han, J.-A.; Kim, Y.-M.; Ha, K.-S. Analysis of Protein Interactions on Protein Arrays by a Novel Spectral Surface Plasmon Resonance Imaging. *Biosens. Bioelectron.* **2006**, *21*, 1521–1528.
17. Bertoncello, P.; Forster, R. J. Nanostructured Materials for Electrochemiluminescence (ECL)-Based Detection Methods: Recent Advances and Future Perspectives. *Biosens. Bioelectron.* **2009**, *24*, 3191–3200.
18. Wang, J. Nanomaterial-Based Electrochemical Biosensors. *Analyst* **2005**, *130*, 421–426.
19. Zhong, W. Nanomaterials in Fluorescence-Based Biosensing. *Anal. Bioanal. Chem.* **2009**, *394*, 47–59.
20. Anker, J. N.; Hall, W. P.; Lyandres, O.; Shah, N. C.; Zhao, J.; Van Duyne, R. P. Biosensing with Plasmonic Nanosensors. *Nat. Mater.* **2008**, *7*, 442–453.
21. Han, X.; Zhao, B.; Ozaki, Y. Surface-Enhanced Raman Scattering for Protein Detection. *Anal. Bioanal. Chem.* **2009**, *394*, 1719–1727.
22. Hutter, E.; Fendler, J. H. Exploitation of Localized Surface Plasmon Resonance. *Adv. Mater.* **2004**, *16*, 1685–1706.
23. Lyon, L. A.; Musick, M. D.; Natan, M. J. Colloidal Au-Enhanced Surface Plasmon Resonance Immunosensing. *Anal. Chem.* **1998**, *70*, 5177–5183.
24. He, L.; Musick, M. D.; Nicewarner, S. R.; Salinas, F. G.; Benkovic, S. J.; Natan, M. J.; Keating, C. D. Colloidal Au-Enhanced Surface Plasmon Resonance for Ultrasensitive Detection of DNA Hybridization. *J. Am. Chem. Soc.* **2000**, *122*, 9071–9077.
25. Hutter, E.; Pileni, M.-P. Detection of DNA Hybridization by Gold Nanoparticle Enhanced Transmission Surface Plasmon Resonance Spectroscopy. *J. Phys. Chem. B* **2003**, *107*, 6497–6499.
26. Hayashida, M.; Yamaguchi, A.; Misawa, H. High Sensitivity and Large Dynamic Range Surface Plasmon Resonance Sensing for DNA Hybridization Using Au-Nanoparticle-Attached Probe DNA. *Jpn. J. Appl. Phys.* **2005**, *44*, 1544–1546.
27. Yao, X.; Li, X.; Toledo, F.; Zurita-Lopez, C.; Gutova, M.; Momand, J.; Zhou, F. Sub-attomole Oligonucleotide and p53 cDNA Determinations *via* a High-Resolution Surface Plasmon Resonance Combined with Oligonucleotide-Capped Gold Nanoparticle Signal Amplification. *Anal. Biochem.* **2006**, *354*, 220–228.
28. Huang, X.; Tu, H.; Zhu, D.; Du, D.; Zhang, A. A Gold Nanoparticle Labeling Strategy for the Sensitive Kinetic Assay of the Carbamate-Acetylcholinesterase Interaction by Surface Plasmon Resonance. *Talanta* **2009**, *78*, 1036–1042.
29. Grigorenko, A. N.; Gleeson, H. F.; Zhang, Y.; Roberts, N. W.; Sidorov, A. R.; Panteleev, A. A. Antisymmetric Plasmon Resonance in Coupled Gold Nanoparticles as a Sensitive Tool for Detection of Local Index of Refraction. *Appl. Phys. Lett.* **2006**, *88*, 124103-3.
30. Lyon, L. A.; Musick, M. D.; Smith, P. C.; Reiss, B. D.; Peña, D. J.; Natan, M. J. Surface Plasmon Resonance of Colloidal Au-Modified Gold Films. *Sens. Actuators, B* **1999**, *54*, 118–124.
31. Law, W.-C.; Markowicz, P.; Yong, K.-T.; Roy, I.; Baev, A.; Patskovsky, S.; Kabashin, A. V.; Ho, H.-P.; Prasad, P. N. Wide Dynamic Range Phase-Sensitive Surface Plasmon Resonance Biosensor Based on Measuring the Modulation Harmonics. *Biosens. Bioelectron.* **2007**, *23*, 627–632.
32. Hooper, I. R.; Rooth, M.; Sambles, J. R. Dual-Channel Differential Surface Plasmon Ellipsometry for Bio-chemical Sensing. *Biosens. Bioelectron.* **2009**, *25*, 411–417.
33. Law, W.-C.; Yong, K.-T.; Baev, A.; Hu, R.; Prasad, P. N. Nanoparticle Enhanced Surface Plasmon Resonance

Biosensing: Application of Gold Nanorods. *Opt. Express* **2009**, *17*, 19041–19046.
34. Etchegoin, P. G.; Le Ru, E. C.; Meyer, M. An Analytic Model for the Optical Properties of Gold. *J. Chem. Phys.* **2006**, *125*, 164705-3.
35. de Kossodo, S.; Houba, V.; Grau, G. E. Assaying Tumor Necrosis Factor Concentrations in Human Serum a WHO International Collaborative Study. *J. Immunol. Methods* **1995**, *182*, 107–114.
36. Szlosarek, P.; Charles, K. A.; Balkwill, F. R. Tumour Necrosis Factor-α as a Tumour Promoter. *Eur. J. Cancer* **2006**, *42*, 745–750.
37. Dalaveris, E.; Kerenidi, T.; Katsabeki-Katsafli, A.; Kiropoulos, T.; Tanou, K.; Gourgoulianis, K. I.; Kostikas, K. VEGF, TNF-α and 8-Isoprostane Levels in Exhaled Breath Condensate and Serum of Patients with Lung Cancer. *Lung Cancer* **2009**, *64*, 219–225.
38. Liu, X.; Dai, Q.; Austin, L.; Coutts, J.; Knowles, G.; Zou, J.; Chen, H.; Huo, Q. A One-Step Homogeneous Immunoassay for Cancer Biomarker Detection Using Gold Nanoparticle Probes Coupled with Dynamic Light Scattering. *J. Am. Chem. Soc.* **2008**, *130*, 2780–2782.
39. Kabashin, A. V.; Kochergin, V. E.; Beloglazov, A. A.; Nikitin, P. I. Phase-Polarisation Contrast for Surface Plasmon Resonance Biosensors. *Biosens. Bioelectron.* **1998**, *13*, 1263–1269.
40. Grigorenko, A. N.; Nikitin, P. I.; Kabashin, A. V. Phase Jumps and Interferometric Surface Plasmon Resonance Imaging. *Appl. Phys. Lett.* **1999**, *75*, 3917–3919.
41. Kabashin, A. V.; Patskovsky, S.; Grigorenko, A. N. Phase and Amplitude Sensitivities in Surface Plasmon Resonance Bio and Chemical Sensing. *Opt. Express* **2009**, *17*, 21191–21204.
42. Ho, H. P.; Lam, W. W.; Wu, S. Y. Surface Plasmon Resonance Sensor Based on the Measurement of Differential Phase. *Rev. Sci. Instrum.* **2002**, *73*, 3534–3539.
43. Sau, T. K.; Murphy, C. J. Seeded High Yield Synthesis of Short Au Nanorods in Aqueous Solution. *Langmuir* **2004**, *20*, 6414–6420.